Effect of Internal Friction on Biofilament Dynamics

Michael G. Poirier* and John F. Marko*,†

University of Illinois at Chicago, 845 West Taylor Street, Chicago, Illinois 60607-7059

(Received 16 May 2001; published 16 May 2002)

We consider *biofilaments*—flexible multimolecule structures common in cell biology—and show how "internal" friction associated with either conformational fluctuations or with fluid flow through narrow pores inside the filaments can dominate the external hydrodynamic friction usually considered to be the main energy dissipation process. The signature of this is wave-number–independent relaxation time of bending fluctuations. Preliminary experimental data for bending fluctuations of single folded (mitotic) chromosomes display these dynamics.

DOI: 10.1103/PhysRevLett.88.228103 PACS numbers: 87.16.Sr, 07.10.Cm, 47.50.+d

Flexible polymers usually have dynamics dominated by hydrodynamic drag on the monomers [1,2]. Polymer theory is at present being extended to describe *biofilaments,* for example, double-standard DNA (dsDNA) [3], actin [4], intermediate filaments [5], chromosomes [6], composite fibers such as dsDNA coated with RecA protein [7], or semiflexible virus particles [8]. These biofilaments are many atoms thick, and are consequently stiff, with persistence lengths much larger than their widths. Current theory of biofilament bending dynamics focuses on thermal fluctuation and external hydrodynamic dissipation [9].

This paper examines the effect of additional, "internal" dissipation, e.g., due to internal conformational rearrangements. Our result is that below a characteristic length scale, dissipation can dominate over hydrodynamic friction, making bending mode relaxation times independent of wave number q. This is distinct from the usual result $\tau \sim 1/q^4$ obtained when external hydrodynamic damping dominates [9]. We also give preliminary evidence for these peculiar dynamics using measurements of bending fluctuations of whole mitotic chromosomes. Mitotic chromosomes are large ($\approx 2 \times 2 \times 20$ μm in size), soft but still elastic filaments [6] with large internal friction [10].

The energy of a filament of length L slightly bent from its straight equilibrium configuration is the integral of its curvature squared. To harmonic order in the transverse displacements as a function of contour length $\mathbf{u}(s)$ this is [11]

$$E = \frac{B}{2}\int_0^L ds\left(\frac{d^2\mathbf{u}}{ds^2}\right)^2 = \frac{B}{2L}\sum_q q^4|\mathbf{u}_q|^2, \qquad (1)$$

where the last term is in terms of Fourier modes $\mathbf{u}_q = \int ds\, e^{iqs}\mathbf{u}(s)$. For a filament with uniform and circular cross section, the bending modulus B (dimensions energy $\times$ length) is related to the Young modulus Y and filament cross-section radius r through $B = \pi Y r^4/4$. In thermal equilibrium,

$$\langle u_q^\alpha u_{-q}^\beta\rangle = \frac{k_B T L}{Bq^4}\,\delta^{\alpha\beta}, \qquad (2)$$

where α and $\beta = 1, 2$ refer to the two components of $\mathbf{u}$. We focus on small-amplitude fluctuations occurring over filament segments L short compared to the persistence length B/k_BT.

The bending dynamics may be described with a Langevin equation [9]

$$B\frac{\partial^4\mathbf{u}}{\partial s^4} + \eta\frac{\partial\mathbf{u}}{\partial t} + \eta' r^4\frac{\partial}{\partial t}\frac{\partial^4\mathbf{u}}{\partial s^4} = \mathbf{n}(s,t). \qquad (3)$$

The first term of (3) accounts for the elastic restoring force from the energy of (1). The second term is the usual hydrodynamic drag force associated with motion of the filament cross section through the surrounding fluid of viscosity η (nonlocal hydrodynamic interactions may be included; see Ref. [9]). The final $\mathbf{n}$ term is random thermal noise with delta-function time correlations. Dropping the η' term of (3) gives the usual dynamical theory of filament fluctuations [9], with a bending mode relaxation time $\tau_q \approx \eta/Bq^4$.

The η' term in (3) describes the effect of internal dissipation; η' itself has dimensions of viscosity. To see where η' comes from, consider the free viscous relaxation of an initially stretched elastic rod, ignoring external hydrodynamic friction and inertial terms. The extension strain $\Delta L/L = \epsilon$ of the rod relaxes according to $\eta'\partial\epsilon/\partial t + Y\epsilon = 0$, where η' (units of viscosity) describes the internal friction which opposes instantaneous relaxation, and where Y is the Young modulus which drives the relaxation. The relaxation time η'/Y is determined by balance of elastic and frictional forces. The rate of energy dissipation in a volume V of the rod is $(\partial E/\partial t)_{\text{friction}} = -V\eta'(\partial\epsilon/\partial t)^2$.

Bending of this rod with local curvature κ generates stretching which is inhomogeneous across the rod cross section, with extension towards the outside edge and compression towards the inside edge. The average of the strain squared across the rod cross section is just $\langle\epsilon^2\rangle_{\text{cross-section}} = \kappa^2 r^2/4$. This identification is familiar from the connection between the usual elastic bending energy of a rod and the integral of its stretching free energy:

$$E_{\text{bending}} = \frac{B}{2}\int_0^L ds\,\kappa^2 = \frac{\pi Y r^2}{2}\int_0^L ds\langle\epsilon^2\rangle_{\text{cross-section}}\,. \tag{4}$$

The same identification allows us to write the rate of energy dissipation associated with the internal friction η':

$$\left(\frac{\partial E}{\partial t}\right)_{\text{friction}} = -\frac{\pi}{8}\,\eta' r^4\int_0^L ds\left(\frac{\partial \kappa}{\partial t}\right)^2. \tag{5}$$

Thus the rate of energy dissipation is proportional to the squared rate of change of local curvature. The energy dissipation rate can be used to find the equation of motion (3), following the Lagrangian formulation of frictional forces [12] [note that a factor of $\pi/4$ from (5) is suppressed in Eq. (3) and below, for clarity of formulas].

A simple mechanical model can give an alternate justification of the energy dissipation rate (5), and therefore of the equation of motion (3). Consider a filament of cross-sectional radius r, the exterior of which is a flexible cylindrical envelope filled with a highly viscous liquid medium of viscosity η'. Running down the center of the tube is a backbone with static bending modulus B. If the time rate of change of curvature is $d\kappa/dt$, then flow of the liquid from the inside edge to the outside edge must occur. Near the middle of the rod, the velocity of this radial flow will be $v \approx r^2 d\kappa/dt$ (relative to the backbone), while at the edges of the rod, the fluid velocity must be zero. Therefore the velocity gradient in the liquid will be $r d\kappa/dt$, and the time rate of energy dissipation per length of rod will be $\approx \eta' r^4 (d\kappa/dt)^2$, essentially (5).

The above arguments amount to description of a biofilament as a thin piece of viscoelastic solid. One way to obtain a large η' is to have slow structural fluctuations, e.g., reptation of entangled polymers, or conformational changes which cross large energy barriers. A second way to obtain a large η', which is relevant to filaments with gel-like internal structure, is the large dissipation associated with the flow of the surrounding fluid of viscosity η through narrow pores. For pores of diameter δ extending across the cross section of a filament, the energy dissipation rate per length is $\approx \eta (r^6/\delta^2)(d\kappa/dt)^2$. This reduces to (5), with an effective internal viscosity $\eta' \approx \eta r^2/\delta^2$. For a filament of gel whose radius r is large compared to the diameter of the gel pores, the effective internal viscosity η' can greatly exceed the viscosity η of the fluid which surrounds and fills the filament.

After Fourier transformation with respect to contour length and time, the equation of motion (3) becomes

$$(Bq^4 + i\eta\omega + i\eta' r^4 q^4 \omega)\mathbf{u}_{q\omega} = \mathbf{n}_{q\omega}\,, \tag{6}$$

leading to the correlation function

$$\langle|\mathbf{u}_{q\omega}|^2\rangle = \frac{\langle|\mathbf{n}_{q\omega}|^2\rangle}{B^2 q^8 + (\eta + \eta' r^4 q^4)^2\omega^2}\,. \tag{7}$$

Choosing delta-function time correlations for $\mathbf{n}(s,t)$ means that $\langle|\mathbf{n}_{q\omega}|^2\rangle$ is a function of q only. Fourier transforming (7) back to equal times must recover (2), which fixes the noise correlation. The bending mode correlations follow as

$$\langle u^\alpha_{q,\omega} u^\beta_{-q,-\omega}\rangle = \frac{2k_B T L(\eta + \eta' r^4 q^4)}{B^2 q^8 + \omega^2(\eta + \eta' r^4 q^4)^2}\,\delta^{\alpha\beta}. \tag{8}$$

The relaxation times of the bending modes are therefore

$$\tau_q = \frac{\eta + \eta' r^4 q^4}{Bq^4}\,. \tag{9}$$

There are two wave-number regimes, separated by a characteristic wave number $q^* = (\eta/\eta')^{1/4}/r$. For long wavelengths, or $q \ll q^*$, the decay times are those of a stiff polymer damped by external hydrodynamic friction, $\langle|\mathbf{u}_{q\omega}|^2\rangle \propto 1/(B^2q^8 + \eta\omega^2)$, with mode relaxation times $\tau_q = \eta/(Bq^4)$. In the opposite small-wavelength limit, $q \gg q^*$, internal dissipation dominates and the correlator is $\langle|\mathbf{u}_{q\omega}|^2\rangle \propto q^{-4}[\omega^2 + B^2/(\eta'^2 r^8)]^{-1}$. In this limit, the relaxation time is *wave-number independent,* $\tau_q = \eta' r^4/B$.

We have preliminary evidence for this wave-number independence of bending relaxation time, from single mitotic chromosomes. We remove folded chromosomes from mitotic (dividing) cells; for our purposes they are elastic rods of cross-section radius $r \approx 1\ \mu$m and length $\leq 20\ \mu$m. Previous experiments have established $Y \approx 500$ Pa [6], and $\eta' \approx 100$ kg/(m · sec) [10]. Since $\eta'/\eta \approx 10^5$, bending relaxation times should be constant for modes with wavelengths up to $2\pi(\eta'/\eta)^{1/4} r \approx 100\ \mu$m. Since this is longer than the chromosomes themselves, we expect all bending modes to relax with the same lifetime $\approx \eta'/Y \approx 0.3$ sec. The observed fluctuations are mainly due to thermal excitation of the smallest–wave-number bending mode ($q \approx \pi/2L$ [13]), so our strategy is to study modes of different q using different-length chromosomes.

Experiments were done using micromanipulated glass micropipettes and an inverted microscope (Olympus IX-70, 60X 1.35 NA objective). A single chromosome was anchored at one end into a pipette of i.d. 2 μm; time series of images were then recorded [6,10]. Digital image analysis was used to track motion of the chromosome edge with $\approx$10 nm precision. Fluctuations were recorded at positions between chromosome tip and pipette (Fig. 1a). We report three experiments on chromosomes with tip-to-pipette lengths of 7, 16.5, and 18.5 μm.

Figure 1b shows time series for amplitude $u(s)$ at a few points along the chromosome of length $L = 18.5\ \mu$m. The amplitudes are very small near the pipette, but grow rapidly as one moves toward the free end. Circles in Fig. 2 (inset) show that the amplitude squared follows the equilibrium law $\langle u^2(s)\rangle \approx k_B T s^3/B$. (Note only one of the two transverse components of $\mathbf{u}$ are measured.) For this chromosome, $B = 3 \times 10^{-22}$ J · m.

Figures 1c and 1d show the 7.0 μm chromosome, and its fluctuation time series near its tip, and near the pipette. As expected, the tip fluctuation amplitude is smaller than

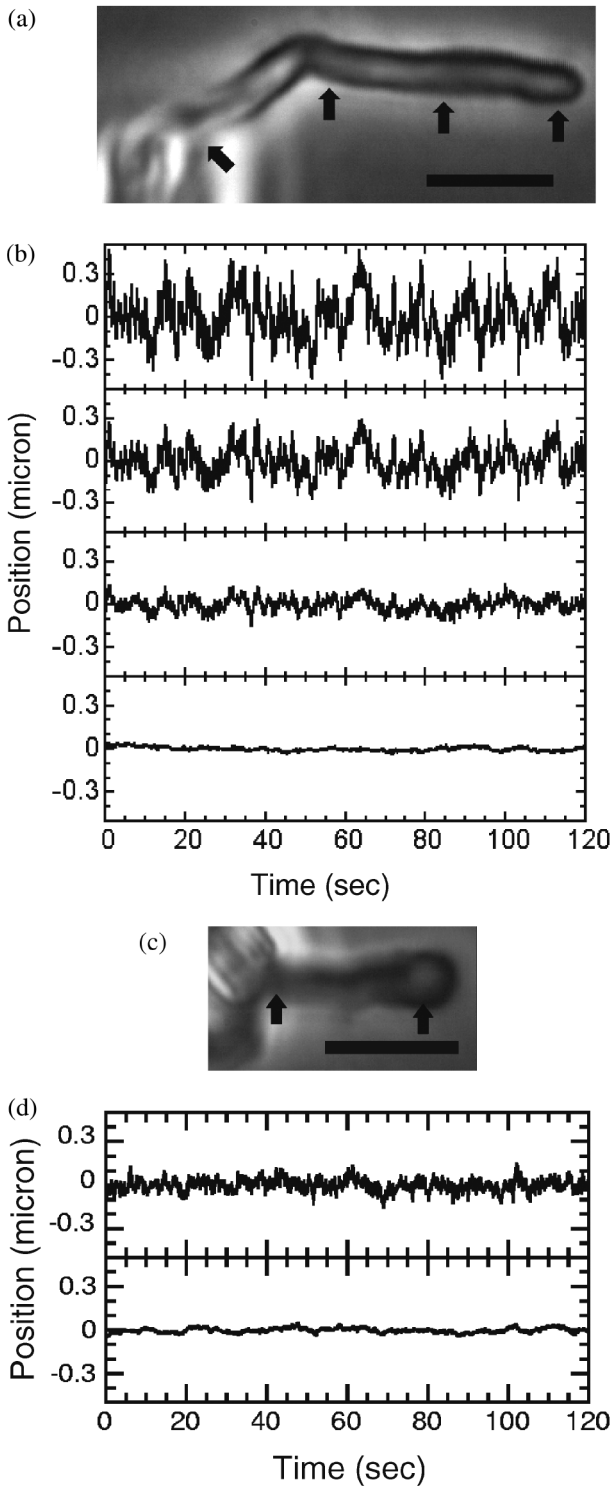

FIG. 1. (a) Micromanipulated chromosome attached at one end to a glass micropipette, with other end free. Total length of chromosome portion outside pipette is 18.5 μm. Bar is 5 μm. (b) Time series for amplitude u observed at a few points along the single mitotic chromosome of (a). The time series shown were measured at the points indicated by arrows in (a). Fluctuation amplitude grows with distance s from the anchored end. (c) Shorter 7.0 μm chromosome attached to glass pipette. Bar is 5 μm. (d) Time series for fluctuations of shorter chromosome of (c) measured at the two points indicated by arrows in (c). Note that the characteristic time of fluctuations is similar to that of the long chromosome of (a),(b).

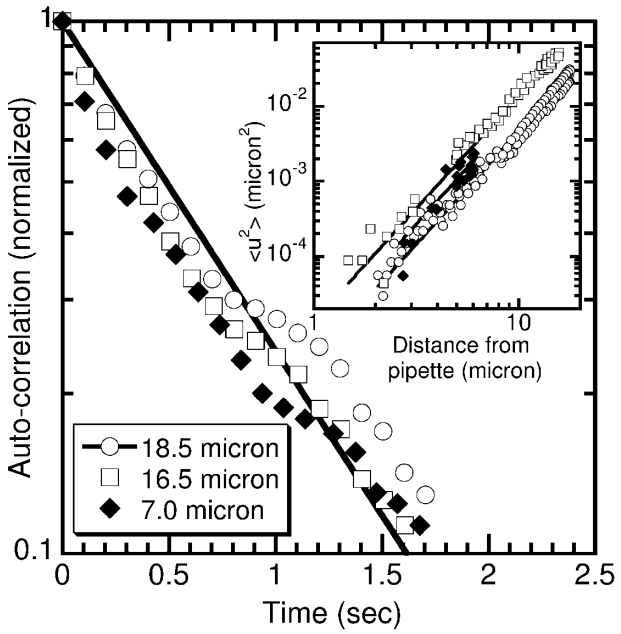

FIG. 2. Inset: Mean-squared amplitude $\langle u^2 \rangle$ for time series as in Fig. 1, versus length from anchored end, shows a cubic power law, as expected theoretically for thermal fluctuations of an elastic rod. The proportionality constant determines the bending modulus B (see text). Diamonds, squares, and circles show results for 7.0-, 16.4-, and 18.5-μm-long chromosomes. The bending moduli (lines) were found to be $B = 1.5 \times 10^{-22}$, 1.0×10^{-22}, and 3.0×10^{-22} J · m, respectively. Following acquisition of bending fluctuation data, Young moduli were directly measured in stretching experiments [6,10] to be $Y = 400$, 500, and 1000 Pa, respectively. Main figure: autocorrelation functions for the free-end fluctuations of three chromosomes are independent of chromosome length. The 7.0 μm (diamonds) and 18.5 μm (circles) correlation functions come from the top time series of Figs. 1b and 1d, respectively. The solid curve indicates the exponential $e^{-t/\tau}$ with $\tau = 0.7$ sec, the approximate time scale expected in the internal-viscosity-dominated regime of Eq. (9).

that of Fig. 1b. The diamonds of Fig. 2 (inset) indicate a bending modulus close to that of the chromosome of Fig. 1a. Squares of Fig. 2 (inset) show similar data for a third chromosome of length 16.5 μm. The equilibrium fluctuations are all consistent with (2), with similar bending moduli.

The time series of Figs. 1b and 1d have similar fluctuation lifetimes. Plots of autocorrelation functions of the tip (largest) fluctuations for the three chromosomes (Fig. 2) show the correlation time to be nearly length independent. If external hydrodynamic damping were the only dissipation mechanism [i.e., if $\eta' = 0$ in (9)], the correlation time for the fluctuations of Fig. 1d should be $(7.0/18.5)^4 \approx 0.02$ of that of Fig. 1b. Instead, the fluctuation lifetime is nearly independent of chromosome length, and therefore of bending mode wave number as expected from (9) for the η'-dominant case.

Further exploration of these effects might be best done using man-made soft filaments of more tailorable structure and physical properties than whole chromosomes. Although chromosomes have well-defined elastic properties,

there is sample-to-sample variation of moduli (see Fig. 2 caption). A more chemically controlled system would allow more tightly quantitative study of internal viscosity effects, which we anticipate should be found in a broad range of soft filaments. As an example, single actin filaments ($r \approx 3$ nm, $B \approx 7 \times 10^{-26}$ J · m [4]) are thought to have internal conformational rearrangement times $\approx 10^{-9}$ sec [14]. This suggests $\eta' \approx B\tau_0/r^4 \approx 1$ kg/m · sec, i.e., $\eta'/\eta \approx 1000$. Therefore, internal viscosity effects likely occur for single actin filaments, only at difficult-to-observe [15] ≈10 nm length scales. However, thicker actin bundles, or cytoskeletal stress filaments, might show internal viscosity effects at more easily accessible length and time scales.

The internal viscosity effects presented here are analogous to internal friction effects discussed for flexible polymers with a single-bond backbone [16]. For flexible polymers, relaxation processes proposed as the origin of internal friction include energy barriers to backbone conformational change. By contrast, the internal friction of this paper has its origin in either relatively large-scale, slow conformational rearrangements of the filament interior, or in hydrodynamic dissipation associated with flow through gel pores. Biofilaments with intermediate (≈30 nm) thicknesses should provide experimental systems for exploration of internal viscosity effects. These effects may also be relevant to thin shells of soft materials such as biological membranes "decorated" with relatively thick layers of proteins or other biopolymers [17].

Illuminating discussions with F. C. MacKintosh are gratefully acknowledged. This research was supported by the Whitaker Foundation through a Biomedical Engineering Research Grant, the NSF through Grant No. DMR-9734178, the Research Corporation, and the Johnson and Johnson Focused Giving Program.

*Department of Physics.
†Department of Bioengineering.

[1] M. Doi and S. F. Edwards, *Theory of Polymer Dynamics* (Oxford University Press, Oxford, 1988), pp. 91–99.
[2] P.-G. de Gennes, *Scaling Concepts in Polymer Physics* (Cornell University Press, Ithaca, NY, 1979), pp. 165–173.
[3] J. F. Marko and E. D. Siggia, Macromolecules **28**, 8759 (1995).
[4] F. Gittes, B. Mickey, J. Nettleton, and J. Howard, J. Cell Biol. **120**, 923 (1993).
[5] M. Hohenadl, T. Storz, H. Kirpal, K. Kroy, and R. Merkel, Biophys. J. **77**, 2199 (1999).
[6] M. Poirier, S. Eroglu, D. Chatenay, and J. F. Marko, Mol. Biol. Cell. **11**, 269 (2000).
[7] M. Hegner, S. B. Smith, and D. Bustamante, Proc. Natl. Acad. Sci. U.S.A. **96**, 10 109 (1999).
[8] F. G. Schmidt, B. Hinner, E. Sackmann, and J. X. Tang, Phys. Rev. E **62**, 5509 (2000).
[9] L. Harnau and P. Reineker, Phys. Rev. E **60**, 4671 (1999).
[10] M. G. Poirier, A. Nemani, P. Gupta, S. Eroglu, and J. F. Marko, Phys. Rev. Lett. **86**, 360 (2001).
[11] L. D. Landau and E. M. Lifshitz, *Theory of Elasticity* (Pergamon Press, Oxford, 1986), pp. 67–70 and 135–137.
[12] L. D. Landau and E. M. Lifshitz, *Mechanics* (Pergamon Press, Oxford, 1976), pp. 74–77.
[13] For "free-clamped" boundary conditions relevant to our setup, the normal modes are close to, but not exactly simple Fourier modes; see C. H. Wiggins, D. Riveline, A. Ott, and R. E. Goldstein, Biophys. J. **74**, 1043 (1998).
[14] E. M. Cruz and T. D. Pollard, Biochemistry **12**, 14 054 (1996).
[15] A. Palmer, J. Xu, S. C. Kuo, and D. Wirtz, Biophys. J. **76**, 1063 (1999).
[16] A. Arbe, M. Monkenbusch, J. Stellbrink, D. Richter, B. Farago, K. Almdal, and R. Faust, Macromolecules **34**, 1281 (2001).
[17] E. Helfer, S. Harlepp, L. Bourdieu, J. Robert, F. C. MacKintosh, and D. Chatenay, Phys. Rev. Lett. **85**, 457 (2000).